ELSEVIER

Chemistry & Biology 8 (2001) 357–368

Chemistry & Biology

www.elsevier.com/locate/chembiol

Research Paper

The three-dimensional structure of human granzyme B compared to caspase-3, key mediators of cell death with cleavage specificity for aspartic acid in P1

Jennifer Rotonda [a,*], Margarita Garcia-Calvo [a], Herb G. Bull [a], Wayne M. Geissler [b], Brian M. McKeever [a], Christopher A. Willoughby [c], Nancy A. Thornberry [a], Joseph W. Becker [a]

[a] *Department of Endocrinology and Chemical Biology, Merck Research Laboratories, P.O. Box 2000, Rahway, NJ 07065-0900, USA*
[b] *Department of Molecular Endocrinology, Merck Research Laboratories, P.O. Box 2000, Rahway, NJ 07065-0900, USA*
[c] *Department of Medicinal Chemistry, Merck Research Laboratories, P.O. Box 2000, Rahway, NJ 07065-0900, USA*

Received 10 October 2000; revisions requested 8 December 2000; revisions received 23 February 2001; accepted 27 February 2001
First published online 22 March 2001

Abstract

Background: Granzyme B, one of the most abundant granzymes in cytotoxic T-lymphocyte (CTL) granules, and members of the caspase (cysteine aspartyl proteinases) family have a unique cleavage specificity for aspartic acid in P1 and play critical roles in the biochemical events that culminate in cell death.

Results: We have determined the three-dimensional structure of the complex of the human granzyme B with a potent tetrapeptide aldehyde inhibitor. The Asp-specific S1 subsite of human granzyme B is significantly larger and less charged than the corresponding Asp-specific site in the apoptosis-promoting caspases, and also larger than the corresponding subsite in rat granzyme B.

Conclusions: The above differences account for the variation in substrate specificity among granzyme B, other serine proteases and the caspases, and enable the design of specific inhibitors that can probe the physiological functions of these proteins and the disease states with which they are associated. © 2001 Published by Elsevier Science Ltd.

Keywords: Autoimmunity; Cell death; Crystal structure; Drug design; X-ray

1. Introduction

Cytotoxic lymphocytes (CLs) are important mediators of cell-mediated immunity, where they are responsible for the destruction of virally infected and transformed cells via two distinct apoptotic mechanisms [1,2]. One involves ligation of Fas ligand to its receptor on target cells, which results in engagement of an apoptotic cascade mediated by members of the caspase family of cysteine proteases. An alternate pathway involves granzymes, a family of serine proteases contained within the cytoplasmic granules of CLs, and the pore-forming protein, perforin. According to the current model for granule-mediated apoptosis, killing involves degranulation and subsequent transfer of these proteases into the cytoplasm of the target cell, where they rapidly induce apoptosis [3]. Several lines of evidence suggest that granzyme B is the predominant protease involved in this latter pathway. First and most compelling, CLs from granzyme B-deficient mice do not efficiently kill target cells [4]. Second, granzyme B and perforin alone can induce apoptosis in target cells [5]. Finally, granzyme B is the most abundant protease contained within cytoplasmic granules [6,7]. Granzyme B-induced cell death appears to be mediated primarily via activation of caspases [8,9]. However, there is mounting evidence that granzyme B can also kill cells via a caspase-independent pathway [10,11]. Indeed, this serine protease and the caspases appear to cleave some of the same cellular substrates, resulting in the demise of the cells [11,12]. This mechanism has

Abbreviations: CL, cytotoxic lymphocyte; RNKP-5, rat natural killer protease-5; MMCP-8 and RMCP-8, mouse and rat mast cell protease-8; RMCP-9, rat mast cell protease-9

* Correspondence: Jennifer Rotonda; E-mail: rotonda@merck.com

1074-5521/01/$ – see front matter © 2001 Published by Elsevier Science Ltd.
PII: S1074-5521(01)00018-7

Fig. 1. (A) Ribbon plot of human granzyme B. The view (referred to as standard orientation) is towards the active site cleft, which runs left to right across the molecular surface. The Ac-IEPD-CHO inhibitor is depicted as a red ball-and-stick model. (B) Stereoview of optimal superposition of the Cα-structures of granzyme B (green, the bound structure of Ac-IEPD-CHO is in gold) and cathepsin G (silver). The view is the standard view as in (A). Landmark residues are identified by amino acid sequence numbers. (C) The amino acid sequences of human granzyme B and human cathepsin G aligned by matching residues that have similar secondary structures or conformation in the aligned three-dimensional structures of the two proteins. Residues in helices are beneath the cyan rectangles; β-strands, red rectangles. Lowercase letters represent residues for which no electron density is evident. To facilitate comparison between granzyme B and cathepsin G, the amino acid residues of granzyme B are identified by the sequence numbers of the homologous residues in cathepsin G in this alignment. The numbering scheme for this family of serine proteases is traditionally based on the zymogen, chymotrypsinogen. (Activation of granzyme B involves several proteolytic cleavages generating an active protease containing a new N-terminal Ile 16.) Granzyme B sequence-specific insertions are indicated by the additions of letters to the cathepsin G sequence numbers. Asterisks indicate the 220 residue Cα's with similar conformations that were used to align the structures. The poorly defined loop (Asp 36A, Gln 36B, Lys 37 and Ser 38), the two granzyme B-specific insertions (Pro 145A and Arg 172A) and Tyr 245 (no electron density) were excluded from the alignment.

→

presumably evolved to facilitate killing of cells infected with viruses that encode caspase inhibitors.

Granzyme B and the caspase family members are the only proteases that have been unequivocally established to be involved in cell death. Despite their distinct catalytic mechanisms, they share a novel and stringent specificity for aspartic acid in the P1 position [13,14]. The granzyme B optimal tetrapeptide recognition motif (P4–P1), IEPD, is also similar to that of caspases involved in the initiation of apoptosis (caspase-8, caspase-9), presumably reflecting their common role in the activation of downstream caspases such as caspase-3, which is activated via cleavage at an IETD site [14,15]. In contrast to these similarities, there are also striking differences in the substrate recognition properties of these enzymes. For example, caspases cleave tetrapeptides and macromolecules with comparable, high efficiency [15]. Conversely, granzyme B cleaves tetrapeptide substrates poorly relative to macromolecules, indicating that substrate recognition involves features beyond the (P4–P1) IEPD recognition motif [14,16]. In addition, pro-apoptotic substrates that are common to the caspases and granzyme B are cleaved efficiently by both, but at distinct sites [11]. The crystal structures of several caspases have been determined and provide a rationale for the substrate specificities of these enzymes [17–22]. To understand the structural basis for the similarities and differences in the substrate recognition properties of the caspases and granzyme B, we have determined the three-dimensional crystal structure of human granzyme B. This information may facilitate efforts to design selective inhibitors that can be used to further probe the distinct biological roles of these enzymes, and to explore their potential value as therapeutic targets.

2. Results and discussion

2.1. Granzyme B structure

We solved the three-dimensional structure of granzyme B in complex with the tetrapeptide aldehyde inhibitor Ac-IEPD-CHO at a nominal resolution of 2.0 Å. A model based on cathepsin G [23], a serine protease with a 56% identity and a 67% similarity to the amino acid sequence of granzyme B, was used to solve the structure of granzyme B by molecular replacement. Analogous to other serine proteases [14,23–26], the granzyme B structure is folded into two six-stranded β-barrels, which are connected by three *trans*-domain segments. Other regular secondary structure elements include a helical loop between Ala 56 and Cys 58, a helix involving residues from Asp 165 to Leu 172, and a long C-terminal helix from Phe 234 to Arg 244 (see Fig. 1). The peptide group between Pro 224 and Pro 225 is in the *cis* conformation in granzyme B as well as in cathepsin G [23], rat mast cell protease II [27], and human chymase [25]. The *cis* proline conformation in human granzyme B orients the positively charged arginine side chain of amino acid 226 into the S1 subsite to interact optimally with the negatively charged P1 aspartic acid of the inhibitor. The above Pro 224–Pro 225 pair is part of a shortened segment, Xaa 221–Xaa 224–Pro 225 (residues 222 and 223 are missing), that is common for this subfamily [28] of serine proteases. In the longer segments of human leukocyte elastase, bovine chymotrypsinogen and bovine β-trypsin, Pro 225 is in the typical *trans* conformation when residue 224 is not a proline [23]. Using the human granzyme B sequence as a query, a computer search was conducted against sequences available in public databases. Of the top 500 protease sequences resulting from this query, the Xaa 221–Xaa 224–Pro 225–Arg 226 motif (based on homology modeling) was only found in human, mouse and rat granzyme B, rat granzyme J (rat natural killer protease-5, RNKP-5), mouse and rat mast cell protease-8 (MMCP-8 and RMCP-8) and rat mast cell protease-9 (RMCP-9). As shown in Table 1, human and mouse granzyme B have the Xaa 221–Pro 224–Pro 225–Arg 226 motif and have a P1 specificity for aspartic acid. Interestingly, rat granzyme B with a Xaa 221–Thr 224–Pro 225–Arg 226 motif also has P1 Asp specificity [14], implying that Pro 225 is in the *cis* conformation in the shortened loop. The recently published structure of rat granzyme B also contains the *cis* conformation of Pro 225 in the shortened loop [29]. Granzyme J, MMCP-8, RMCP-8, and RMCP-9 also have the Xaa 221–Xaa 224–Pro 225–Arg 226 motif but residue 216, which is typically a glycine forming two of the three anti-parallel β-structure-like hy-

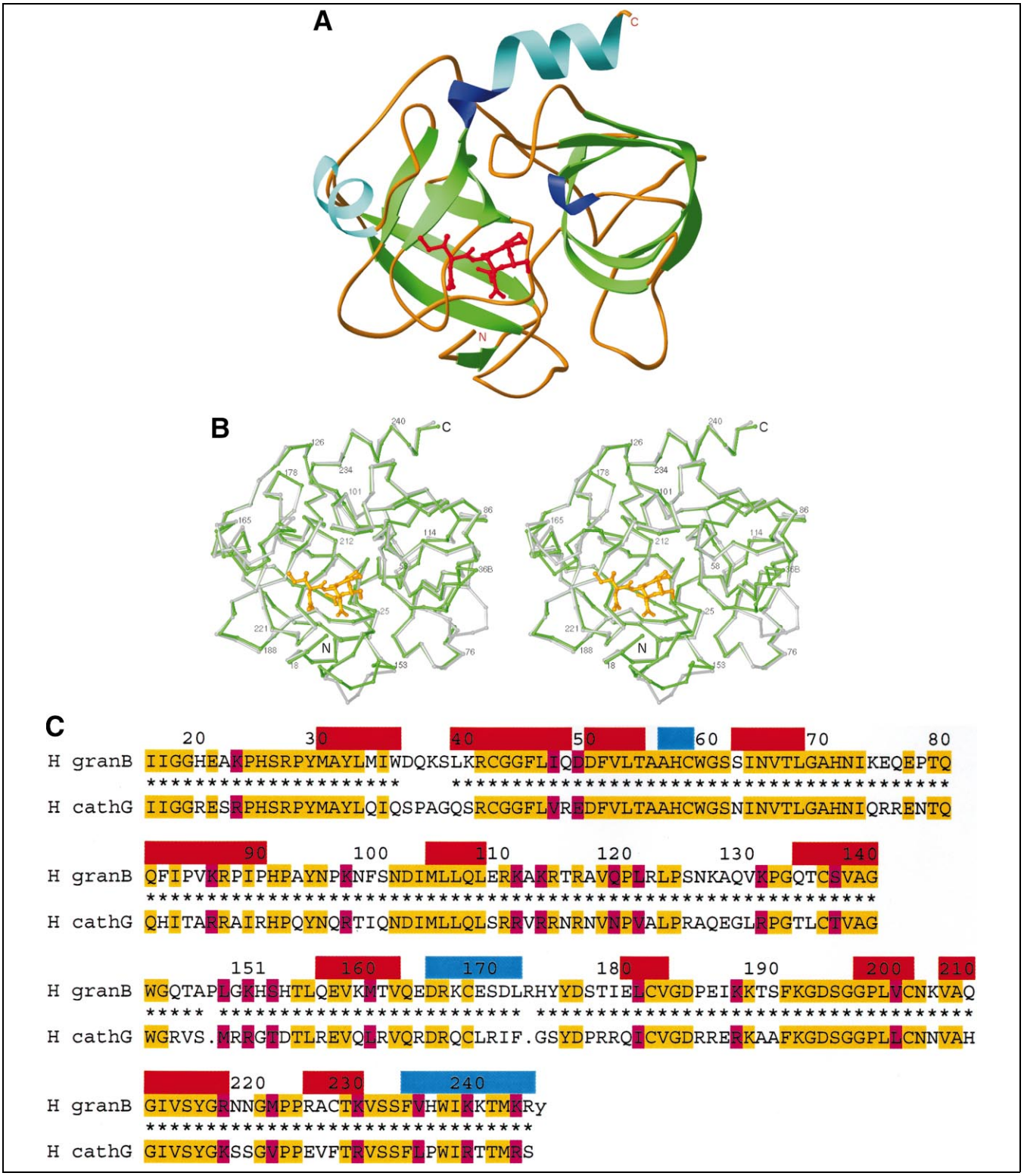

drogen bonds between the inhibitor backbone and the enzyme (see Fig. 2), is an arginine. This large, positively charged side chain will point right into the S1 subsite causing the side chain of Arg 226 to most likely displace the water molecules from the extended area of the S1 subsite (see Fig. 3). Similar to the caspases (Fig. 2), the S1 subsite with two arginines, including granzyme J, MMCP-8, RMCP-8, and RMCP-9, will presumably be Asp-specific as well.

As with related serine proteases, the catalytic residues of human granzyme B, His 57, Asp 102 and Ser 195, are located at the junction of the two β-barrels with the active

Table 1
Comparison of specific residues of serine proteases with a Xaa 221–Xaa 224–Pro 225–Arg 226 motif

	216	221	224	225	226	228	P1 specificity
Human granzyme B	Gly	Met	Pro	Pro	Arg	Cys	Asp
Mouse granzyme B	Gly	Ser	Pro	Pro	Arg	Phe	Asp
Rat granzyme B	Gly	Ser	Thr	Pro	Arg	Phe	Asp
Rat granzyme J	Arg	Thr	Pro	Pro	Arg	Phe	unknown
Rat mast cell protease-9	Arg	Thr	Pro	Pro	Arg	Phe	unknown
Rat mast cell protease-8	Arg	Thr	Leu	Pro	Arg	Phe	unknown
Mouse mast cell protease-8	Arg	Thr	Leu	Pro	Arg	Phe	unknown

site cleft perpendicular to this junction. Similarly, the N-terminal amino acid of the mature granzyme B, Ile 16, lies in the interior of the molecule, where its ammonium group forms an internal salt bridge with the side chain carboxylate of Asp 194. This salt bridge formation is linked to the creation of the oxyanion hole and the functional S1 pocket in the mature protease [26]. When the refined granzyme B and cathepsin G structures are aligned on 220 residues with similar secondary structure or conformation (Fig. 1B), the average difference between equivalent Cα atoms is 0.50 Å (r.m.s. 0.40 Å). The poorly resolved loop, composed of residues Asp 36A, Gln 36B, Lys 37 and Ser 38, was not included in the overall alignment since the corresponding loop in cathepsin G has no electron density [23]. The two insertions into the granzyme B sequence, Pro 145A and Arg 172A, determined by the align-

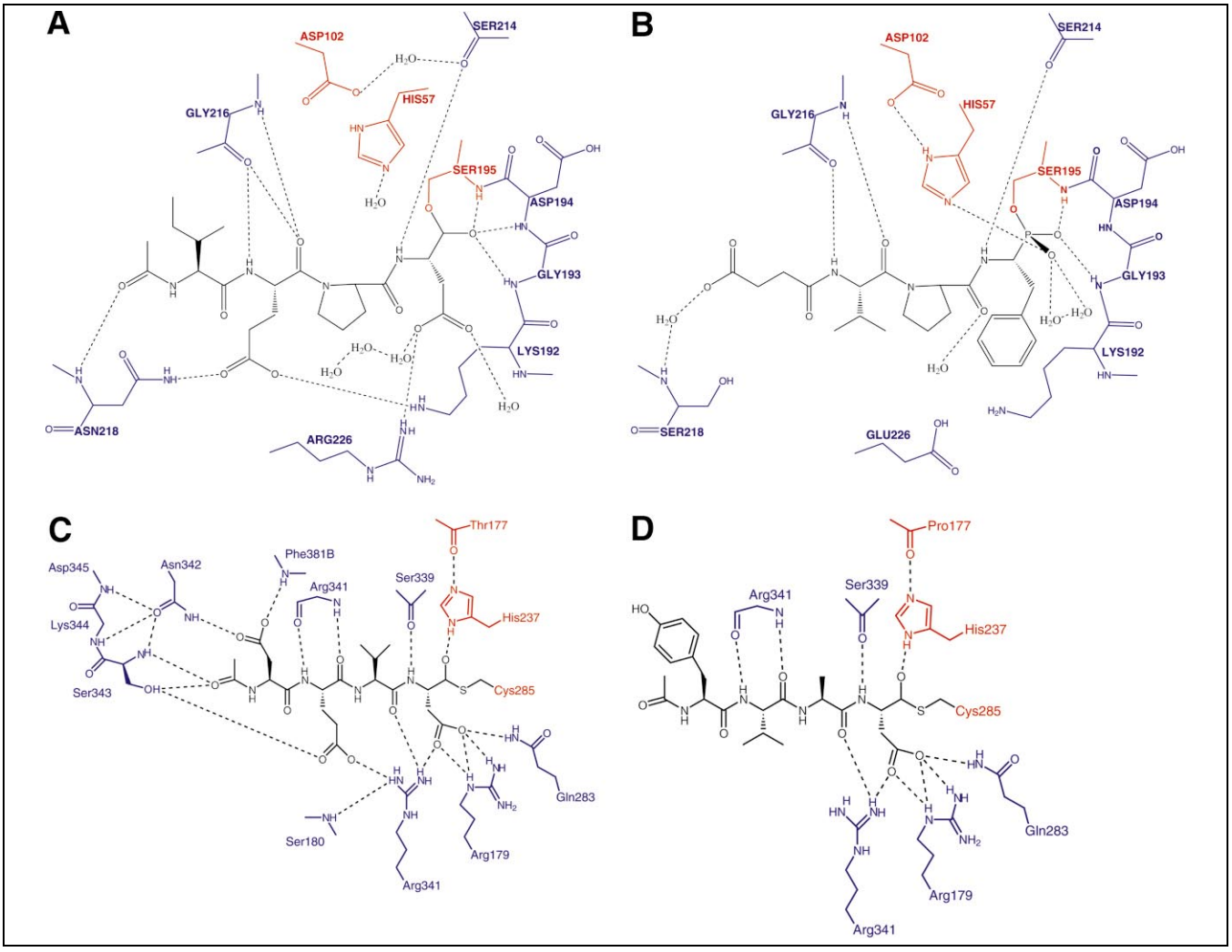

Fig. 2. (A) Hydrogen bonds and other polar interactions between Ac-IEPD-CHO ($K_i = 80$ nM) and human granzyme B. Orange residues are the catalytic triad, purple residues are protein, black residues are inhibitor. (B) Between Suc–Val–Pro–Phe(P)–(OPh)2 (irreversible transition state analogue inhibitor) and human cathepsin G [23]. (C) Between Ac-DEVD-CHO ($K_i = 0.35$ nM) and human caspase-3 [19]. (D) Between Ac-YVAD-CHO ($K_i = 0.76$ nM) and human caspase-1 [19].

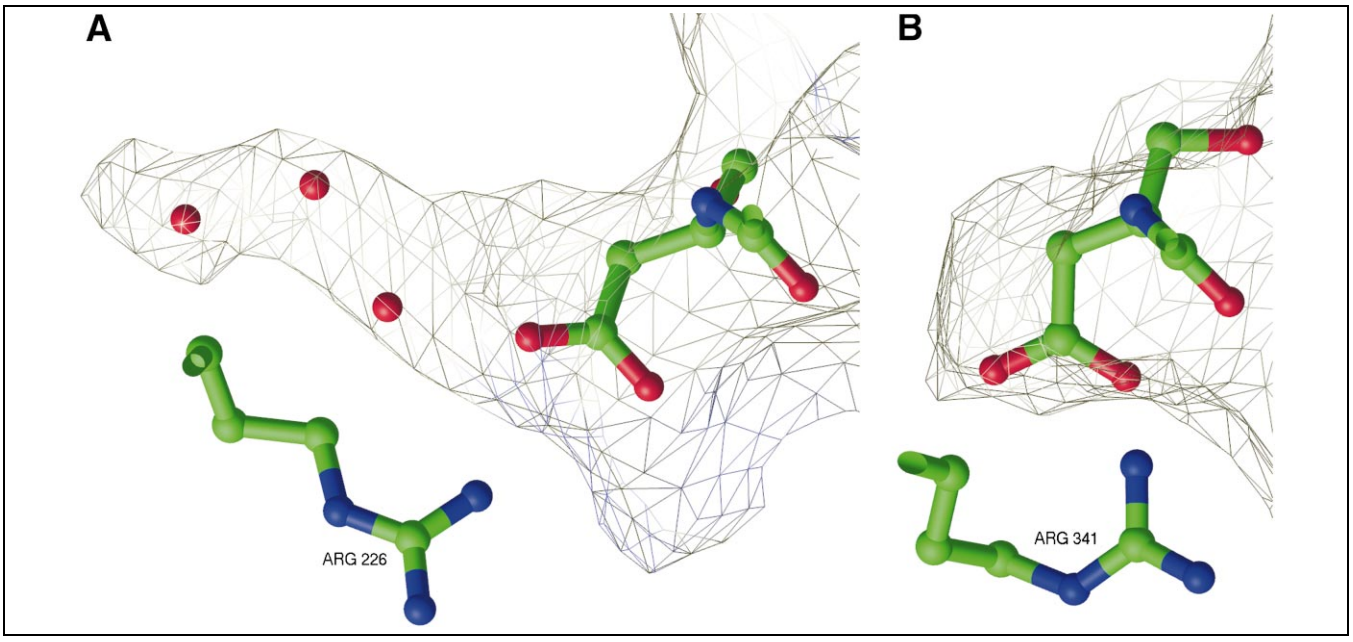

Fig. 3. Comparison of the S1 subsites. The surface of the protein is represented by mesh and the entry into the binding pocket is from the right of the picture. (A) The aspartic acid side chain of Ac-IEPD-CHO bound to granzyme B includes three water molecules in the S1 subsite. (B) The P1 aspartic acid side chain of Ac-DEVD-CHO bound to caspase-3.

ment of the sequences and the structures, and the C-terminal Tyr 245 for which no electron density is evident, were also not included in the overall alignment. The 13 arginines and 19 lysines of granzyme B are solvent-exposed except for Arg 226 in S1. These residues produce large positively charged surface patches mostly distant from the active site. Since there are only nine solvent-exposed glutamate and seven solvent-exposed aspartate residues, the resulting surface of the enzyme is relatively basic. Two additional aspartic acids, Asp 102, a member of the catalytic triad, and Asp 194, salt-linked to Ile 16, are not solvent-exposed.

Mass spectral analysis of human recombinant granzyme B identifies one major peak at 27 466 Da (see Section 4). Since the combined mass of the 227 amino acids defined by sequence analysis only accounts for 25 512 Da, granzyme B has approximately two glycosylation sites accounting for the 1954 Da mass difference. The electron density clearly identifies two Asn-linked, solvent-exposed glycosylation sites extending from the side chains of Asn 65 and Asn 98. Only the first N-acetyl glucosamine (GlcNAc) residue of the N-linked carbohydrate is clearly visible off of Asn 65 while six residues (two GlcNAc, one fucose, three mannose) of the complex N-linked glycans [30] are bound to the side chain of Asn 98. These seven residues account for 1312 Da. The electron density becomes very weak beyond these residues because of crystallographic disorder. Difference density maps also identify five tetrahedrally coordinated zinc ions. Zinc sulfate was used as an additive during crystallization producing zinc ions as artifacts of crystallization. Zinc is not required for substrate binding (M. Garcia-Calvo, unpublished results). Four of the five zinc ions are coordinated by at least one Nε2 atom of the imidazole ring of a histidine residue. The carboxylate oxygens of aspartic and glutamic acids coordinate the fifth zinc ion. Three of the five zinc ions are coordinated by amino acid side chains from symmetry-related molecules of granzyme B in complex with Ac-IEPD-CHO. The other two ions are solvent-exposed. Four of the five zinc sites are coordinated by at least one water molecule. The observed tetrapeptide aldehyde inhibitor of granzyme B sits in the active site groove on the highly charged surface of the protein in an extended conformation, similar to the P1–P4 residues of the inhibited caspase structures (see Fig. 4). However, the hydrogen bonds and polar interactions involving the aspartic acid at P1 are noticeably different in granzyme B and caspase-3 (see Fig. 2). The well-defined and extensive granzyme B prime subsites, S1′–S3′, are also considerably different from those in the caspases.

2.2. Specificity differences at the S1 and S prime subsites

The tetrapeptide aldehyde inhibitor, Ac-Ile-Glu-Pro-Asp-CHO, is bound in a groove in the enzyme surface (see Fig. 4). The side chains at P1 and P4 project into pronounced depressions in the binding groove where they make numerous interactions with the protein while the P2 and P3 side chains point away from the body of the protein. The hydrogen bonds and other polar interactions between the inhibitor and the protein are shown in Fig. 2. As predicted [14,24], inhibited granzyme B, like cathepsin G, caspase-3 and caspase-1, has three anti-parallel β-structure-like hydrogen bonds between the inhibitor backbone and the enzyme (Fig. 2): granzyme B and cathepsin G, P1

N···Ser 214 O, P3 N···Gly 216 O, and P3 O···Gly 216 N; caspase-3 and caspase-1, P1 N···Ser 339 O, P3 N···Arg 341 O, and P3 O···Arg 341 N. However, there are no hydrogen bonds involving the P2 and P4 carbonyls and the P4 amide of Ac-IEPD-CHO with granzyme B. The absence of these bonds benefits the development of future inhibitors by reducing the number of peptide-like features required for inhibition.

The S1 subsite of granzyme B differs from the model of cathepsin G used for molecular replacement. Cathepsin G has a negatively charged glutamic acid in amino acid position 226 that is off to one side of the S1 site, hydrogen-bonded to the amide nitrogen and carbonyl of Ala 190. The P1 specificity for cathepsin G is Phe. Granzyme B has a positively charged arginine residue that results in a change of both the size and chemical composition of the S1 subsite. Arg 226 in granzyme B forms a partial base to the site and allows an extensive network of waters to form off to one side of the P1 side chain (see Fig. 3). These unique features make S1 Asp-specific and also provide the room necessary to build inhibitors with extensions into this site for improved specificity. When granzyme B and caspase-3 are compared, the amino acid compositions of the corresponding subsites differ significantly in both their overall geometry and their chemical nature. Granzyme B and the caspases are the only known mammalian proteases with a primary specificity for aspartic acid [14,15]. All of the known caspase structures are virtually identical at the S1 subsite suggesting identical modes of substrate recognition and catalytic mechanism [17–22]. The ability of the negatively charged P1 aspartyl side chain of inhibitors and substrates to stabilize the local concentration of the two positive charges of the arginyl side chains in the S1 subsite of these enzymes, is consistent with the near absolute requirement for Asp in P1 [15,19,31]. Although granzyme B has the same primary specificity, its Asp-specific S1 subsite is significantly larger (Fig. 3) and less charged than the corresponding conserved site in the caspases. The granzyme B S1 subsite contains only one positively charged group, Arg 226, in contrast to the two arginine side chains present in the caspase-3 S1 subsite. These subsite differences probably account for the variation in orientation of the P1 aspartic acids in the active sites (Fig. 5A). The P1 aspartic acid side chain of Ac-IEPD-CHO interacts with the guanidinium group of Arg 226 and also forms hydrogen bonds with an extended network of three water molecules within the S1 subsite of granzyme B.

An 'oxyanion hole', which is presumed to stabilize the oxyanion of the reaction intermediates formed during catalysis, is made by the amide nitrogen atoms of Gly 193, Asp 194 and Ser 195. The affinity of peptide aldehyde inhibitors for serine proteases was initially attributed to the ability of these compounds to form a hemiacetal with the active site serine that resembles the transition state in amide bond hydrolysis, with the oxyanion stabilized in the oxyanion hole. In the granzyme B–Ac-IEPD-CHO complex, the aldehyde carbonyl of the P1 aspartic acid forms a hemiacetal with the γ oxygen of the active site Ser 195 of granzyme B (Fig. 5C). The inhibitor of granzyme B appears to bind predominantly in the transition state conformation, with the oxyanion of the hemiacetal stabilized by hydrogen bonds to the amide nitrogens of Gly 193, Asp 194 and Ser 195 but there are indications of disorder. In the alternate conformation, the oxyanion forms a hydrogen bond with the amide nitrogen of Gly 193. Carefully designed refinement experiments on this complex failed to establish definitively either the transition

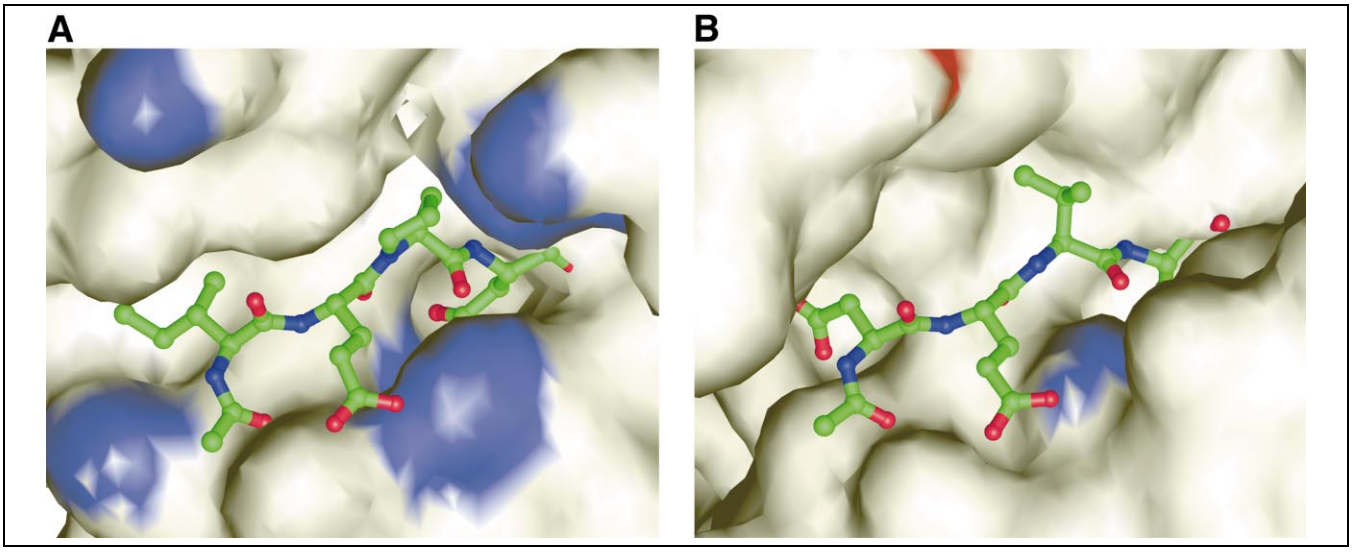

Fig. 4. Comparison of the active sites surfaces of (A) granzyme B (blue represents positive charge; and the red, negative) with Ac-IEPD-CHO (atom color ball-and-stick model) and (B) caspase-3 with Ac-DEVD-CHO. The respective protein complexes were aligned on the four residue Cα's of the inhibitors, producing the average difference between equivalent Cα atoms of 0.38 Å (r.m.s. 0.12 Å). 375 Å^2 of the surface of granzyme B is buried by the inhibitor Ac-IEPD-CHO while 348 Å^2 of the surface of caspase-3 is buried by the inhibitor Ac-DEVD-CHO.

or non-transition state conformation to the exclusion of the other. In parallel refinements, each conformation fitted equally well to electron density maps and to simulated annealing omit maps. Difference electron density maps based on each conformation contained indications suggesting some contribution from the alternate conformation. Disordered binding of peptide aldehyde inhibitors has been observed in some serine proteases, suggesting that this mode of binding may be of some generality [32,33]. Similar experiments [19] on a cysteine protease, caspase-3, also demonstrate disorder in the binding of an inhibitor. Recently, the 1.2 Å structure of human caspase-8 in complex with Ac-IETD-CHO clearly shows that the thiohemiacetal binds in a non-transition state conformation [20].

Combinatorial synthetic substrate libraries and substrate phage display showed the optimal substrate sequence for granzyme B, spanning six subsites, P4–P2′, to be (P4)Ile–Glu–Xaa–Asp↓Xaa–Gly(P2′) with the cleavage at the Asp↓Xaa peptide bond [14]. The definitions of the S1′, S2′, and S3′ subsites in granzyme B are consistent with data demonstrating that the enzyme–substrate interactions C-terminal to the scissile bond are catalytically significant and play a role in determining substrate specificity [14]. Caspase-3 has an extended shallow groove on the surface of the protein representing the S1′ subsite while granzyme B has deep, tunnel-like features defining S1′, S2′, and S3′ subsites. In granzyme B, S1′ is a large hydrophobic pocket formed by the disulfide bridge between Cys 58 and Cys 42, the carbon atoms of the side chain of Lys 40, and the side chain of Ile 35. This pocket is large enough to fit a tryptophan. The prime subsites continue with a narrow corridor, representing S2′, to another network of waters forming the hydrophilic S3′ subsite (Fig. 5D). This narrow corridor, between the side chain of Arg 41, the main chain of Gly 193, and the side chain of His 151 is consistent with the specificity for glycine at P2′. Our structure of granzyme B has identified a large hydrophilic S3′ subsite formed by the main chain atoms between Arg 41 and Gly 43, Val 138 and Gly 142, and Gly 193 and Pro 198 and covered by the side chains of Tyr 32, Trp 141 and Met 30. This 'subsite' is filled with four well-defined water molecules and may actually be more than one subsite.

2.3. *Other interactions with inhibitor*

The S4 subsite of granzyme B is a shallow hydrophobic depression formed by aromatic rings (Tyr 174 and Tyr 215) and the side chain of Leu 172. However, the surface edges of the S4 subsite are composed of solvent-exposed arginines (Arg 217 and Arg 172A). Our structure, with an Ile in P4, and the P4 peptide specificity profile [15] demonstrates that there is not enough room for a P4 phenylalanine. In contrast, the S4 subsite of caspase-3 is a narrow pocket that closely envelops the P4 Asp side chain. This pocket is sterically constricted by the side chains of Trp 348 and Phe 381B and the required P4 aspartic acid makes specific polar interactions with Phe 381A and Asn 342 (which extends its hydrogen bond network by additional polar interactions with the amide nitrogens of Ser 343, Lys 344 and Asp 345). Thus, the S4 subsite of granzyme B is less constricted and more hydrophobic than the corresponding subsite in caspase-3.

The side chains of the preferred P3 glutamic acid residues in both granzyme B and caspase-3 point away from the body of the protein. The P3 amide nitrogen and carbonyl of these proteins form anti-parallel β-structure-like hydrogen bonds with the main chain of their respective protein. The side chain of P3 Glu of granzyme B interacts with both Asn 218 and Lys 192, stabilizing the lysine side chain along the edge of the groove of the binding site. Similarly, P3 Glu in caspase-3 makes a salt link to the side chain of Arg 341 and a polar interaction with the side chain of Ser 343, consistent with the specificity of the enzyme at this site.

In the caspase-3–Ac-DEVD-CHO complex, the side chain of the P2 valine points away from the body of the protein and lies against a hydrophobic wall of the groove and adjacent to the side chain of Tyr 338. In granzyme B, the aromatic ring of Phe 99 forms a hydrophobic wall at the S2 subsite and the catalytic His 57 is flipped up (χ_1 rotation), out of its catalytic formation with Ser 195 and Asp 102, adapting an conformation previously observed in other serine protease structures [34]. In granzyme B, the P2 proline points away from the body of the protein and makes no specific interactions with the protein. Just beyond the pentameric pyrrolidine ring of the proline, there is a pocket formed by the side chains of Phe 99, Tyr 94, Asp 102, His 57 and the main chain of Pro 96. Extensions to this ring may improve binding to granzyme B. This proline induces a slight kink in the tetrapeptide inhibitor of granzyme B allowing the P1 aspartic acid to reach its optimal conformation in the S1 subsite (Fig. 5A) [23,25,35].

2.4. *Comparison of the structures of human and rat granzyme B*

The recently published structure of the complex between rat granzyme B and the macromolecular inhibitor ecotin [29] is quite similar to the present structure in its overall features. When the structures are aligned, the r.m.s. deviation between 217 structurally related α-carbon atoms is 0.59 Å. There are a few differences in the composition of specific subsites because of sequence differences between the human and rat proteins. In S2, Phe 99 of human granzyme B is an isoleucine in rat. In S2′, His 151 is a tyrosine in rat while Arg 41 is a lysine. The differences in S1 are particularly striking. Cys 228 of human granzyme B is a phenylalanine in the rat enzyme (Table 1). This change results in a significantly larger S1 subsite in the human

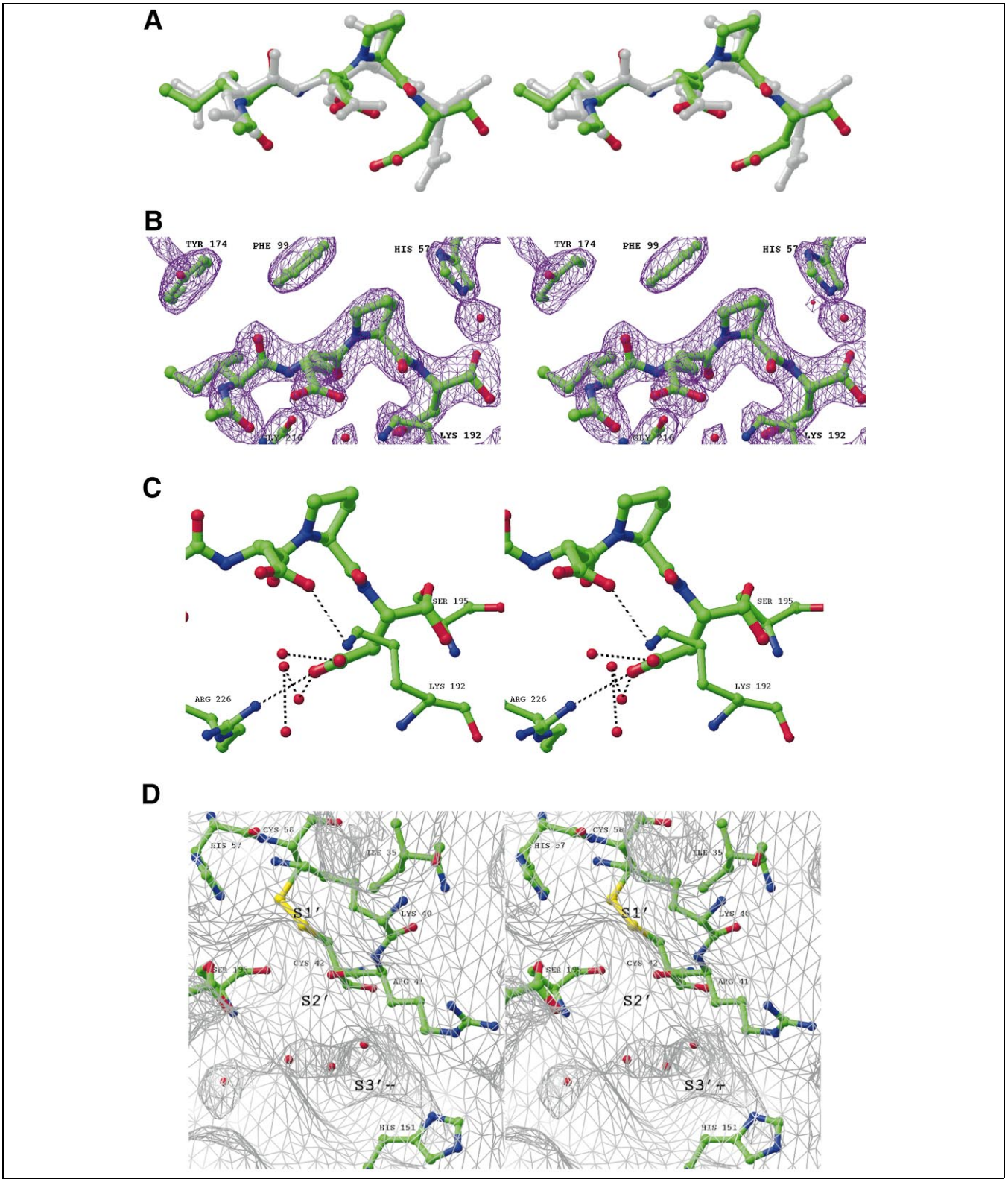

protein. While this site is a narrow pit, approximately 7 Å in diameter and 9 Å deep in the rat enzyme, the Phe–Cys sequence difference results in an extra channel in the human S1, extending towards Val 138 and approximately 7 Å in length. This added volume contains three ordered water molecules in the human enzyme. Also, the specific polar interactions between the Asp side chain of the substrate/inhibitor and Arg 226 differ in detail. In the human complex, there is a single interaction between Oδ2 of the P1 aspartic acid and Nη2 of Arg 226, while in the rat complex there is a bidentate interaction involving both Oδ's of the P1 Asp and the Nε and Nη2 atoms of Arg 226. These

Fig. 5. (A) Stereoview of overlay of the bound conformation of Ac-IEPD-CHO (atom color ball-and-stick model) from the granzyme B complex and Ac-DEVD-CHO (silver ball-and-stick model) from the caspase-3 complex. The respective inhibitors were aligned as in Fig. 4. (B) Electron density in the region of the bound inhibitor. ($2F_o-F_c$) electron density map calculated with the final refined phases is superimposed on the refined model. (C) The S1 subsite. The carbonyl of P1 forms a hemiacetal with the γ oxygen of the active site Ser 195. The P1 aspartic acid side chain interacts with the main chain amide nitrogen of Lys 192 and the guanidinium group of Arg 226 (that also forms the base of S1). There is an extended network of three water molecules in S1. (The terminal side chain nitrogen of Lys 192 is H-bonded to the P3 glutamic acid side chain.) S1 contains only one positively charged group, in contrast to the two arginine side chains in the caspase S1 subsites. (D) The prime subsites of granzyme B. The granzyme B surface is represented by the silver mesh. S1′ is a large hydrophobic pocket adjacent to a relatively small S2′ and a large S3′ which is filled with another network of water molecules. S1′ is a large hydrophobic pocket formed by a disulfide bridge (Cys 42–Cys 58), the carbon atoms of the side chain of Lys 40 and the side chain of Ile 35. This prime site continues with a narrow corridor (formed by Arg 41 and His 151) to another network of waters forming the hydrophilic S3′ subsite (follow the four waters in the prime subsites from right to left).
←

differences may arise both from specific sequence differences between the rat and human enzymes as well as the fact that rat granzyme B is in complex with a cleaved substrate, while human granzyme B is inhibited by a tetrapeptide aldehyde. The S1 subsite differences between rat and human granzyme B will affect the binding of non-peptidyl inhibitors. Phe 228, which points directly into S1, is found in rat and mouse granzyme B, MMCP-8, RMCP-8, and RMCP-9 (Table 1). Only human granzyme B has an extended S1 subsite with three water molecules and a cysteine at residue 228. Thus, a specific inhibitor's structure activity relationship with rat granzyme B may not be predictive of its ability to inhibit human granzyme B.

3. Significance

The three-dimensional structure of granzyme B is generally similar in secondary and tertiary structure to that of trypsin-like serine proteases. Despite this superficial similarity, there are profound differences in the S1 subsite that account for the distinct macromolecular specificities and different biological functions of these enzymes. The strict requirement for aspartic acid in the P1 position of substrates and inhibitors of granzyme B, a specificity not previously seen in serine proteases, is confirmed by the geometry and the chemical nature of this subsite. In addition, the results presented here provide a structural basis for the design of highly specific inhibitors of human granzyme B. The absence of hydrogen bonds involving the P2 and P4 carbonyls and the P4 amide eliminates the number of peptide bonds necessary to build this inhibitor. The extensions possible from P2 and/or into S1 as well as the S′ subsites should improve our inhibitors and aid in the identification of the appropriate targets for therapeutic intervention.

4. Materials and methods

4.1. Granzyme B production

Plasmid pMelBac and the TA cloning kit (pCR2.1) were purchased from Invitrogen (Carlsbad, CA, USA). The Bac-to-Bac baculovirus expression system and all cell culture supplies were from Life Technologies (Gaithersburg, MD, USA). The full length human granzyme B clone was a generous gift from Dr. Chris Bleakley [36]. A vector was generated for secreted protein expression in the Bac-to-Bac system. The honeybee melittin secretion signal was amplified from pMelBac by PCR with primers 5′-GTGT **AGA TCT** ATG AAA TTC TTA GTC AAC G-3′ and 5′-TTC AGC AGA GTC GAC TCC AAG-3′. The amplified product contained a *Bgl*II site upstream of the melittin secretion signal and spanned the multiple cloning site of the vector. The fragment was digested with *Bgl*II and *Eco*RI and subcloned into *Bam*HI and *Eco*RI digested pFastBac. The resulting vector was designated pSecBac. Tagged human granzyme B was cloned into pSecBac in two sequential steps. Firstly, mature granzyme B was amplified from Dr. Bleakley's clone by PCR with primers 5′-GGATCC **ATC GAA GGT CGT** ATC ATC GGAGGACAT-GAGGCC-3′ and 5′-AAG CTT TTA GTA GCG CTT CAT GGT CTT CTT TAT CC-3′ and cloned into pCR2.1. In the sense primer, the bold type sequence coding for the factor Xa recognition site, Ile–Glu–Gly–Arg, was inserted upstream of isoleucine 21 (referred to as Ile 16 in this paper using the numbering scheme for this family of serine proteases that is traditionally based on the zymogen, chymotrypsinogen), the first amino acid of mature granzyme B. Secondly, hexa-histidine tagged granzyme B was amplified from the granzyme B/pCR2.1 clone by PCR using primers 5′-GGA AGA TCT CAT CAT CAT CAT CAT CAT GGA TCC ATC GAA GGT CGT ATC-3′ and 5′-CCT GAA TTC TTA GTA GCG TTT CAT GGT CTT CTT TAT CC-3′. The amplified product contained a *Bgl*II site upstream of the hexa-histidine tag and contained the factor Xa recognition sequence. This fragment was digested with *Bgl*II and *Eco*RI and subcloned into *Bam*HI and *Eco*RI digested pSecBac. The completed vector generated a recombinant baculovirus in Gibco BRL's Bac-to-Bac system, which would produce a secreted, 6-histidine tagged granzyme B. For protein expression, *sf9* cells were grown to a density of 1.5×10^6 cells ml^{-1} in Grace's medium (Cat. 11605-094) supplemented with 10% fetal calf serum and penicillin–streptomycin–glutamine (Cat. 10378-024). Prior to the addition of virus, cells were centrifuged at $1000\times g$ for 15 min and resuspended to the same density in fresh growth medium containing recombinant viral stock and SP Sepharose beads (4 ml resin per liter of culture). After 72 h of induction at 27°C, the resin was collected in a 50 μ nylon mesh (PGC Scientifics), extensively washed with 50 mM MES–NaOH, 0.3 M NaCl, pH 6.6

and poured into a column. The protein was eluted using a linear gradient (0.3–1.0 M) of NaCl. Since the eluted granzyme B is inactive, aliquots of the fractions were incubated overnight with factor Xa and the activity of the resulting granzyme B was measured in a continuous fluorometric assay using Ac-IETD-AMC as a substrate, similar to the previously described assays for the caspases [37–39]. Fractions containing granzyme B activity were identified, combined and concentrated and then diluted in 20 mM Tris–HCl, pH 8.0. The sample was readjusted to a final pH 8.0, $CaCl_2$ (3 mM final concentration) and factor Xa (Pharmacia, 10 units per mg of protein) was added, and incubated for 18 h at room temperature to generate active granzyme B. Under these conditions, complete cleavage is achieved. The recombinant granzyme B was purified from the cleavage mixture using a 1 ml HiTrap SP column (Pharmacia). The yield can be as much as 4–5 mg of active, purified granzyme B per liter of culture as measured using the above fluorometric assay. Mass spectral analysis identifies one major peak at 27 466 Da (other components of 27 320 Da and 26 630 Da were also consistently observed). Since the combined mass of the 227 amino acids defined by sequence analysis only accounts for 25 511.58 Da, we concluded that preparations of recombinant granzyme B purified with this method are more homogeneous and less glycosylated than preparations of native granzyme B purified from NK cell granules (data not shown). Nevertheless, the resulting enzyme is indistinguishable from native enzyme with regard to kinetic parameters for inhibition by Ac-IEPD-CHO and other inhibitors.

4.2. Crystallization, data measurement, structure solution

The granzyme B–Ac-IEPD-CHO complex was crystallized by hanging-drop vapor diffusion. 0.5 ul drops of protein–inhibitor solution (12.2 mg ml^{-1} in 20 mM Tris–HCl pH 8.0, 200 mM NaCl) were mixed with an equal volume of precipitant solution (25% PEG monomethyl ether-550 (v/v), 0.10 M MES pH 6.5, 10 mM $ZnSO_4$, 12 mM $ZnCl_2$) and incubated at room temperature over a reservoir of 24% w/v PEG-3350, 12.8% v/v PEG MME-550, 50 mM MES pH 6.5, 5 mM $ZnSO_4$, and 6 mM $ZnCl_2$. The crystals belong to the orthorhombic space group $P2_12_12_1$ with $a = 48.87$, $b = 75.08$, $c = 80.26$ Å. Three-dimensional diffraction data extending to a resolution of 2.0 Å were collected at beamline 17-ID in the IMCA-CAT facilities at the Advanced Photon Source (see acknowledgments) using monochromatic wavelength of 1.0 Å and a 165 mm Mar Research CCD image plate detector. These data were processed with the HKL2000 software package [40]. 163 991 observations of 19 956 unique reflections were merged with an *R*-factor of 4.4%. The structure was solved by molecular replacement, using X-PLOR [41] and a model based on cathepsin G [23] (Protein Data Bank [42] entry 1CGH). The current model was constructed by interactive model building [43–45] and refined with X-PLOR and CNX [46] using all diffraction data. The current model was inspected against simulated annealing omit maps [47] and comprises residues 16–244 of the protein, the bound inhibitor, 114 ordered water molecules, five zinc ions and a total of seven residues of the complex N-linked glycans are bound to the side chains of Asn 65 and Asn 98. The electron density becomes very weak beyond these residues because of crystallographic disorder. The *R*-factor of the refined model is 24.7% ($_{R\text{free}} = 27.5\%$) [48] and the stereochemistry is reasonable (r.m.s. deviation of bonds = 0.009 Å, angles = 1.54°). Crystallographic statistics are presented in Table 2. The *R*-factor of the final model is most likely affected by the disorder present in the glycosylation sites. Over 600 Da of the glycosylated granzyme B complex are not capable of being modeled. Subsequent refinements of other inhibited granzyme B complexes (data not shown) have extended to a resolution of 1.8 Å thus increasing the number of visible carbohydrate residues and decreasing the *R*-factor significantly. Secondary structures were assigned to granzyme B using the program STRIDE [48]. Special care was taken to establish the chirality at the optical center created by the nucleophilic attack of Ser 195 OH at the P1 carbon atom. After refinement was completed, equivalent models were constructed for each possible configuration at this atom and the two models were refined in parallel with chiral restraints that were identical in magnitude, but opposite in hand. Then, all atoms within 8.0 Å of this atom were deleted from each model and both truncated models were subjected to a 2000 K simulated annealing refinement. Electron density maps and simulated annealing omit electron density maps of this part of the complex were then calculated from both sets of phases and inspected to determine the stereochemistry at this site. The coordinates and structure factors of the granzyme B–Ac-IEPD-CHO complex have been deposited in the Protein Data Bank [42] and the PDB code is 1IAU.

Acknowledgements

We thank Dr. R. Chris Bleackley (Department of Biochemistry, University of Alberta, Edmonton, AB, Canada) for the full length human granzyme B clone. We are grate-

Table 2
Crystallographic data and refinement

Crystals		Data collection		Refinement	
Space group	$P2_12_12_1$	Reflections		R.m.s. deviation	
Unit cell	$a = 48.87$ Å	observed	163 991	of bonds	0.009 Å
	$b = 75.08$ Å	unique	19 956	of angles	1.539°
	$c = 80.26$ Å	completeness	95% to 2.0 Å		
				R_{free}	27.5%
Resolution	2.0 Å	R_{merge}	4.4%	R	24.7%

ful for the advice and expertise of Dr. Antony Rosen (Johns Hopkins University School of Medicine, Baltimore, MD, USA).

Data were collected at beamline 17-ID in the facilities of the Industrial Macromolecular Crystallography Association Collaborative Access Team (IMCA-CAT) at the Advanced Photon Source. These facilities are supported by the companies of the Industrial Macromolecular Crystallography Association through a contract with Illinois Institute of Technology (IIT), executed through the IIT's Center for Synchrotron Radiation Research and Instrumentation. Use of the Advanced Photon Source was supported by the U.S. Department of Energy, Basic Energy Sciences, Office of Science, under contract no. W-31-109-Eng-38. We sincerely appreciate the assistance of the IMCA staff.

References

[1] E.A. Atkinson, R.C. Bleackley, Mechanisms of lysis by cytotoxic T cells, Crit. Rev. Immunol. 15 (1995) 359–384.
[2] G. Berke, The CTL's kiss of death, Cell 81 (1995) 9–12.
[3] P.A. Henkart, Lymphocyte-mediated cytotoxicity: two pathways and multiple effector molecules, Immunity 1 (1994) 343–346.
[4] J.W. Heusel, R. Wesselschmidt, S. Shresta, J. Russell, T.J. Ley, Cytotoxic lymphocytes require granzyme B for rapid induction of DNA fragmentation and apoptosis in allogeneic target cells, Cell 76 (1994) 977–984.
[5] L. Shi, R.P. Kraut, R. Aebersold, A.H. Greenberg, A natural killer cell granule protein that induces DNA fragmentation and apoptosis, J. Exp. Med. 175 (1992) 553–566.
[6] M. Poe, J.T. Blake, D.A. Boulton, M. Gammon, N.H. Sigal, J.K. Wu, H.J. Zweerink, Human cytotoxic lymphocyte granzyme B. Its purification from granules and the characterization of substrate and inhibitor specificity, J. Biol. Chem. 266 (1991) 98–103.
[7] M.C. Peitsch, J. Tschopp, Granzyme B, Methods Enzymol. 244 (1994) 80–87.
[8] A.J. Darmon, D.W. Nicholson, R.C. Bleackley, Activation of the apoptotic protease CPP32 by cytotoxic T-cell-derived granzyme B, Nature 377 (1995) 446–448.
[9] S.J. Martin, G.P. Amarante-Mendes, L. Shi, T.-H. Chuang, C.A. Casiano, G.A. O'Brien, P. Fitzgerald, E.M. Tan, G.M. Bokoch, A.H. Greenberg, D.R. Green, The cytotoxic cell protease granzyme B initiates apoptosis in a cell-free system by proteolytic processing and activation of the ICE/CED-3 family protease, CPP32, via a novel two-stop mechanism, EMBO J. 15 (1996) 2407–2416.
[10] A. Sarin, M.S. Williams, M.A. Alexander-Miller, J.A. Berzofsky, C.M. Zacharchuk, P.A. Henkart, Target cell lysis by CTL granule exocytosis is independent of ICE/Ced-3 family proteases, Immunity 6 (1997) 209–215.
[11] F. Andrade, S. Roy, D.W. Nicholson, N.A. Thornberry, A. Rosen, L. Casciola-Rosen, Granzyme B directly and efficiently cleaves several downstream caspase substrates: implications for CTL-induced apoptosis, Immunity 8 (1998) 451–460.
[12] D.A. Thomas, C. Du, M. Xu, X. Wang, T.J. Ley, DFF45/ICAD can be directly processed by granzyme B during the induction of apoptosis, Immunity 12 (2000) 621–632.
[13] N.A. Thornberry, S.M. Molineaux, Interleukin-1β converting enzyme: a novel cysteine protease required for IL-1β production and implicated in programmed cell death, Protein Sci. 4 (1995) 3–12.
[14] J.L. Harris, E.P. Peterson, D. Hudig, N.A. Thornberry, C.S. Craik, Definition and redesign of the extended substrate specificity of granzyme B, J. Biol. Chem. 273 (1998) 27364–27373.
[15] N.A. Thornberry, T.A. Rano, E.P. Peterson, D.M. Rasper, T. Timkey, M. Garcia-Calvo, V.M. Houtzager, P.A. Nordstrom, S. Roy, J.P. Vaillancourt, K.T. Chapman, D.W. Nicholson, A combinatorial approach defines specificities of members of the caspase family and granzyme B, J. Biol. Chem. 272 (1997) 17907–17911.
[16] L. Casciola-Rosen, F. Andrade, D. Ulanet, W.B. Wong, A. Rosen, Cleavage by granzyme B is strongly predictive of autoantigen status: implications for initiation of autoimmunity, J. Exp. Med. 190 (1999) 815–825.
[17] K.P. Wilson, J.A. Black, J.A. Thomson, E.E. Kim, J.P. Griffith, M.A. Navia, M.A. Murcko, S.P. Chambers, R.A. Aldape, S.A. Raybuck, Structure and mechanism of interleukin-1 beta converting enzyme, Nature 370 (1994) 270–275.
[18] N.P. Walker, R.V. Talanian, K.D. Brady, L.C. Dang, N.J. Bump, C.R. Ferenz, S. Franklin, T. Ghayur, M.C. Hackett, L.D. Hammill, Crystal structure of the cysteine protease interleukin-1 beta-converting enzyme: a $(p20/p10)^2$ homodimer, Cell 78 (1994) 343–352.
[19] J. Rotonda, D.W. Nicholson, K.M. Fazil, M. Gallant, Y. Gareau, M. Labelle, E.P. Peterson, D.M. Rasper, R. Ruel, J.P. Vaillancourt, N.A. Thornberry, J.W. Becker, The three-dimensional structure of apopain/CPP32, a key mediator of apoptosis, Nat. Struct. Biol. 3 (1996) 619–625.
[20] W. Watt, K.A. Koeplinger, A.M. Mildner, R.L. Heinrikson, A.G. Tomasselli, K.D. Watenpaugh, The atomic-resolution structure of human caspase-8, a key activator of apoptosis, Struct. Fold. Des. 7 (1999) 1135–1143.
[21] H. Blanchard, L. Kodandapani, P.R. Mittl, S.D. Marco, J.F. Krebs, J.C. Wu, K.J. Tomaselli, M.G. Grutter, The three-dimensional structure of caspase-8: an initiator enzyme in apoptosis, Struct. Fold. Des. 7 (1999) 1125–1133.
[22] Y. Wei, T. Fox, S.P. Chambers, J. Sintchak, J.T. Coll, J.M.C. Golec, L. Swenson, K.P. Wilson, P.S. Charifson, The structures of caspases-1, -3, -7 and -8 reveal the basis for substrate and inhibitor selectivity, Chem. Biol. 7 (2000) 423–432.
[23] P. Hof, I. Mayr, R. Huber, E. Korzus, J. Potempa, J. Travis, J.C. Powers, W. Bode, The 1.8 Ang crystal structure of human cathepsin G in complex with Suc-Val-Pro-Phe(P)-(OPh)2: a Janus-faced proteinase with two opposite specificities, EMBO J. 15 (1996) 5481–5491.
[24] M.E.P. Murphy, J. Moult, R.C. Bleackley, H. Gershenfeld, I.L. Weissman, M.N.G. James, Comparative molecular model building of two serine proteinases from cytotoxic T lymphocytes, Proteins Struct. Funct. Genet. 4 (1988) 190–204.
[25] P.J.B. Pereira, Z.-M. Wang, H. Rubin, R. Huber, W. Bode, N.M. Schechter, S. Strobl, The 2.2 Ang crystal structure of human chymase in complex with succinyl-Ala-Ala-Pro-Phe-chloromethylketone: structural explanation for its dipeptidyl carboxypeptidase specificity, J. Mol. Biol. 286 (1999) 163–173.
[26] W. Bode, R. Huber, Structural basis of the endoproteinase–protein inhibitor interaction, Biochim. Biophys. Acta 1477 (2000) 241–252.
[27] S.J. Remington, R.G. Woodbury, R.A. Reynolds, B.W. Matthews, H. Neurath, The structure of rat mast cell protease II at 1.9-A resolution, Biochemistry 27 (1988) 8097–8105.
[28] C. Lutzelschwab, G. Pejler, M. Aveskogh, L. Hellman, Secretory granule proteases in rat mast cells. Cloning of 10 different serine proteases and a carboxypeptidase A from various rat mast cell populations, J. Exp. Med. 185 (1997) 13–29.
[29] S.M. Waugh, J.L. Harris, R.J. Fletterick, C.S. Craik, The structure of the pro-apoptotic protease granzyme B reveals the molecular determinants of its specificity, Nat. Struct. Biol. 7 (2000) 762–765.
[30] D.L. Jarvis, Z.S. Kawar, J.R. Hollister, Engineering N-glycosylation pathways in the baculovirus-insect cell system, Curr. Opin. Biotechnol. 9 (1998) 528–533.
[31] N.A. Thornberry, Y. Lazebnik, Caspases: enemies within, Science 281 (1998) 1312–1316.
[32] L.T. Delbaere, G.D. Brayer, The 1.8 Ang structure of the complex

between chymostatin and *Streptomyces griseus* protease A. A model for serine protease catalytic tetrahedral intermediates, J. Mol. Biol. 183 (1985) 89–103.

[33] C. Ortiz, C. Tellier, H. Williams, N.J. Stolowich, A.I. Scott, Diastereotopic covalent binding of the natural inhibitor leupeptin to trypsin: detection of two interconverting hemiacetals by solution and solid-state NMR spectroscopy, Biochemistry 30 (1991) 10026–10034.

[34] I. Botos, E. Meyer, M. Nguyen, S.M. Swanson, J.M. Koomen, D.H. Russell, E.F. Meyer, The structure of an insect chymotrypsin, J. Mol. Biol. 298 (2000) 895–901.

[35] S. Rehault, M. Brillard-Bourdet, M.A. Juliano, L. Juliano, F. Gauthier, T. Moreau, New, sensitive fluorogenic substrates for human cathepsin G based on the sequence of serpin-reactive site loops, J. Biol. Chem. 274 (1999) 13810–13817.

[36] C.G. Lobe, B.B. Finlay, W. Paranchych, V.H. Paetkau, R.C. Bleackley, Novel serine proteases encoded by two cytotoxic T lymphocyte-specific genes, Science 232 (1986) 858–861.

[37] N.A. Thornberry, H.G. Bull, J.R. Calaycay, K.T. Chapman, A.D. Howard, M.J. Kostura, D.K. Miller, S.M. Molineaux, J.R. Weidner, J. Aunins, K.O. Elliston, J.M. Ayala, F.J. Casano, J. Chin, G.J.-F. Ding, L.A. Egger, E.P. Gaffney, G. Limjuco, O.C. Palyha, S.M. Raju, A.M. Rolando, J.P. Salley, T.-T. Yamin, T.D. Lee, J.E. Shively, M. MacCoss, R.A. Mumford, J.A. Schmidt, M.J. Tocci, A novel heterodimeric cysteine protease is required for interleukin-1-beta processing in monocytes, Nature 357 (1992) 768–774.

[38] D.W. Nicholson, A. Ali, N.A. Thornberry, J.P. Vaillancourt, C.K. Ding, M. Gallant, Y. Gareau, P.R. Griffin, M. Labelle, Y. Lazebnik, Identification and inhibition of the ICE/CED-3 protease necessary for mammalian apoptosis, Nature 376 (1995) 37–43.

[39] M. Garcia-Calvo, E.P. Peterson, D.M. Rasper, J.P. Vaillancourt, R. Zamboni, D.W. Nicholson, N.A. Thornberry, Purification and catalytic properties of human caspase family members, Cell Death Differ. 6 (1999) 362–369.

[40] Z. Otwinowski, W. Minor, Processing of X-Ray Diffraction Data Collected in Oscillation Mode, Academic Press, New York, 1996.

[41] A.T. Brunger, X-PLOR: Version 3.1, a System for X-Ray Crystallography and NMR, Yale University Press, New Haven, CT, 1992.

[42] H.M. Berman, J. Westbrook, Z. Feng, G. Gilliland, T.N. Bhat, H. Weissig, I.N. Shindyalov, P.E. Bourne, The Protein Data Bank, Nucleic Acids Res. 28 (2000) 235–242.

[43] J.S. Sack, CHAIN - a crystallographic modeling program, J. Mol. Graph. 6 (1988) 224–225.

[44] T.A. Jones, J.Y. Zou, S.W. Cowan, M. Kjeldgarrd, Improved methods for binding protein models in electron density maps and the location of errors in these models, Acta Crystallograph. D 47 (1991) 110–119.

[45] G.J. Kleywegt, T.A. Jones, Software for handling macromolecular envelopes, Acta Crystallograph. D 55 (1999) 941–944.

[46] A.T. Brunger, P.D. Adams, G.M. Clore, W.L. DeLano, P. Gros, R.W. Grosse-Kunstleve, J.-S. Jiang, J. Kuszewski, M. Nilges, N.S. Pannu, R.J. Read, L.M. Rice, T. Simonson, G.L. Warren, Crystallography and NMR System: a new software suite for macromolecular structure determination, Acta Crystallograph. D 54 (1998) 905–921.

[47] A. Hodel, S.-H. Kim, A.T. Brunger, Model bias in macromolecular crystal structures, Acta Crystallograph. A 48 (1992) 851–858.

[48] D. Frishman, P. Argos, Knowledge-based protein secondary structure assignment, Proteins Struct. Funct. Genet. 23 (1995) 566–579.